[CANCER RESEARCH 63, 7158–7166, November 1, 2003]

The Gene Expression Response of Breast Cancer to Growth Regulators: Patterns and Correlation with Tumor Expression Profiles

Heather E. Cunliffe, Markus Ringnér, Sven Bilke, Robert L. Walker, Jennifer M. Cheung, Yidong Chen, and Paul S. Meltzer[1]

Cancer Genetics Branch, National Human Genome Research Institute, NIH, Bethesda, Maryland 20892 [H. E. C., R. L. W., J. M. C., Y. C., P. S. M.]; Complex Systems Division, Department of Theoretical Physics, Lund University, SE-223 62 Lund, Sweden [M. R.]; and Advanced Technology Center, National Cancer Institute, Gaithersburg, Maryland 20877 [S. B.]

ABSTRACT

The effects of hormone and growth factor signaling on gene expression contribute significantly to breast tumorigenesis and disease progression; however, the targets of signaling networks associated with deregulated growth are not well understood. We defined the dynamic transcriptional effects elicited in MCF7, T-47D, and MDA-MB-436 breast cancer cell lines by nine regulators of growth and differentiation (17β-estradiol, antiestrogens fulvestrant and tamoxifen, progestin R5020, antiprogestin RU486, all-*trans*-retinoic acid, epidermal growth factor, mitogen-activated protein/extracellular signal-regulated kinase 1/2 inhibitor U0126 and phorbol ester 12-*O*-tetradecanoylphorbol-13-acetate) and compared the patterns of gene regulation to published tumor expression profiles. The complex pattern of response to these agents revealed unexpected relationships between their effects, including a profound overlap in genes regulated by both steroids and epidermal growth factor, and striking overlaps between fulvestrant and all-*trans*-retinoic acid. Estrogen-responsive genes could be divided into two major clusters, only one of which is associated with cell proliferation. Gene ontology analysis was used to highlight functionally distinct biological responses to different mitogens. Significant correlations were identified between several clusters of drug-responsive genes and genes that discriminate estrogen receptor status or disease outcome in patient samples. The majority of estrogen receptor status discriminators were not responsive in our dataset and are therefore likely to reflect underlying differences in histogenesis and disease progression rather than growth factor signaling. This article highlights the overall impact at the gene expression level of diverse regulators of breast cancer growth and links the behavior of breast cancer cells in culture to important clinical properties of human breast tumors.

INTRODUCTION

Steroid hormones and peptide growth factors mediate diverse physiological functions associated with normal growth and differentiation of the mammary gland and also contribute significantly to the development and progression of breast cancer. Specific molecular events that contribute to disease, as well as biological responses to breast cell growth regulators and have been intensively studied, resulting in the development of target-selective therapeutic agents. For example, breast cancers that are ER[2]-positive often respond to 4-OHT and fulvestrant (ICI) that antagonize estrogen receptor signaling. Breast tumors also frequently overexpress members of the epidermal growth factor receptor family of receptor tyrosine kinases, most notably erbB2, which is overexpressed in up to 30% of cases. Moreover, activation of MAPK signaling is significantly increased in up to 50% of breast cancers compared with normal breast epithelium and is associated with poor patient prognosis (1, 2). The majority of these tumors are ER−, suggesting that up-regulated growth factor signaling in these tumors provides an effective alternative to growth stimulation by steroid hormones. In addition to hormone antagonists, there are a number of other agents, which cause growth arrest in cultured breast cancer cells. Phorbol esters such as TPA, which regulates diacylglycerol-dependent signaling via PKC, are known to promote G_1 growth arrest of breast cancer cells (3, 4). This TPA-mediated arrest appears to be associated with raf/extracellular signal-regulated kinase-dependent induction of $p21^{WAF1/CIP1}$ cyclin-dependent kinase inhibitor, as well as antagonism of ER signaling in estrogen-sensitive breast cancer cells (5–7). Synthetic derivatives of atRA are another important class of agents with potent antineoplastic effects in experimental models of breast cancer (8, 9). Retinoids show promise as effective chemopreventive agents (9, 10), heightening interest in understanding the mechanisms by which these agents affect tumor growth and progression.

Our understanding of signal transduction components and their interactions regulating growth and arrest of breast cancer cells is still limited. Microarray technologies provide a powerful method to explore the complexities of transcriptional profiles defined by selected pharmacological mitogens and inhibitors pivotal for breast cancer cell growth. Recently, our laboratory and others (11–17) have used expression arrays to subclassify breast tumors into categories possessing distinct biological and clinical properties. Among the distinctions made to date, the strongest separation is observed between ER+ and ER− tumors. This highlights the question of how genes contributing to the tumor subclassification are associated with a particular hormone or growth factor signal. Because this question is difficult to address using patient samples, we chose an *in vitro* model system using cultured cell lines treated with agents known to induce breast cancer cell mitosis or growth arrest. Human breast tumor cell lines have been used extensively as models of neoplastic disease, and accordingly, their expression profiles provide a frame of reference for assessing the biological significance of expression patterns in a specific tumor (11, 18). There have been several studies of gene expression analysis of breast cancer cells treated with a limited number of growth agonists and antagonists, producing catalogues of responsive genes (19–25). These studies, although valuable, do not address the highly networked nature of signaling components with respect to regulation of gene expression. Individual growth regulators may impact (in a temporally distinct manner) on multiple axes of cell signaling, and conversely, multiple agents impinge on the same signaling cascades. For example, steroid hormones signal to the MAPK and protein kinase A/PKC axes (26–29), which strongly suggests that the gene expression responses to growth factors, steroids, and activators of second messengers may overlap.

In this article, we present a detailed analysis of the observed patterns of gene expression in MCF7, T-47D, and MDA-MB-436 breast cancer cells treated for 2, 8, and 24 h with E2, estrogen antagonists 4-OHT, ICI, a progestin (R5020), an antiprogestin

Received 6/19/03; revised 8/15/03; accepted 8/27/03.

The costs of publication of this article were defrayed in part by the payment of page charges. This article must therefore be hereby marked *advertisement* in accordance with 18 U.S.C. Section 1734 solely to indicate this fact.

[1] To whom requests for reprints should be addressed, at National Human Genome Research Institute, NIH, 50 South Drive, Bethesda MD 20892-8000. Phone: (301) 594-5283; Fax: (301) 402-3281; E-mail: pmeltzer@nhgri.nih.gov.

[2] The abbreviations used are: ER, estrogen receptor-α; CSS, charcoal dextran-treated serum; E2, 17β-estradiol; ICI, ICI 182,780; 4-OHT, 4-hydroxy tamoxifen; atRA, all-*trans*-retinoic acid; EGF, epidermal growth factor; TPA, 12-*O*-tetradecanoyl-phorbol-13-acetate; MAPK, p44/42 mitogen-activated protein kinase; Mek, MAP/ERK kinase; PKC, protein kinase C; EST, expressed sequence tag; MTT, 3-(4,5-dimethylthiazol-2-yl)-2,5-diphenyltetrazolium bromide; GO, Gene Ontology.

RU486, atRA, EGF, a Mek1/2-specific inhibitor (U0126), and a phorbol ester (TPA). We hypothesized that by examining both the unique and interrelated time-sensitive patterns of gene expression and interpreting these in the context of GO and phenotypic response to each agent, we may identify pathways significantly impacted by breast cell growth regulators. We predicted that this study may also reveal individual or related groups of genes representing new candidates to investigate for their involvement in disease progression. The patterns of gene expression found *in vitro* were compared with *in vivo* gene expression profiles previously identified in breast cancer specimens. This comparative analysis reveals a significant association between specific gene clusters and discriminators of hormone receptor status and disease progression in tumor samples.

MATERIALS AND METHODS

Cell Culture and RNA Isolation. Cell lines were obtained from the American Type Culture Collection and maintained at 37°C in 5% CO_2 in RPMI 1640 supplemented with 10% FBS and 1 mM L-glutamine. Before stimulation with E2, R5020, EGF, or TPA, cells were cultured for 48 h in CSS media [phenol red-free MEMα with 10% charcoal/dextran-treated FBS (HyClone), 1 mM L-glutamine and nonessential amino acids]. Reagents are: 10 nM E2 (Sigma); 100 nM 4-OHT (Calbiochem); 100 nM pure antiestrogen ICI (Tocris); 1 μM R5020 (Perkin-Elmer); 1 μM RU486 (Sigma); 1 μM atRA (Sigma); 25 μg/ml EGF (Invitrogen); 10 μM U0126 (Cell Signaling Technology); and 100 nM TPA (Sigma). Cells were treated in parallel with either reagent or vehicle control. At 2, 8, and 24 h, two dishes of cells (one reagent-treated and one control) were harvested for RNA extraction. The control for each pair was the matched reference sample for hybridization. Cells were washed twice with PBS and lysed using TRIzol reagent (Invitrogen). Total RNA was extracted from TRIzol as recommended by the manufacturer, then further purified by addition of an equal volume of 70% ethanol, followed by RNeasy column extraction (Qiagen).

MTT Growth Assays. Quantitation of cell growth rates was determined using the Vibrant MTT cell proliferation kit (Molecular Probes). Cells were seeded in 96-well plates in triplicate and treated with reagent or vehicle control. Growth medium and reagent were replaced at 48-h intervals. Solubilized formazan concentration was determined at absorbance 570 nm.

Immunoblotting. Cells were seeded into 6-well plates and cultured for 48 h in CSS media as described above. Cells were serum starved (CSS media with 0.5% serum) for 24 h before stimulation. Whole cell lysate preparation and immunoblotting were performed as described previously (30). Antibodies were obtained from Cell Signaling Technology and ICN Biomedicals, Inc.

cDNA Microarrays. Microarray slides containing 13,824 sequence-verified cDNA clones (10,536 unique genes) were obtained from the National Human Genome Research Institute/National Institute of Neurological Disorders and Stroke/National Institute of Mental Health microarray core facility. Gene names were listed according to build 154 of the UniGene human sequence collection.[3] Sample labeling and microarray hybridization were conducted as previously described (31, 32) and using standard protocols.[4] Fluorescence scanning and image analysis with DeArray software were performed as described previously (33, 34). Microarray data presented herein is also available.[4] Data from replicate experiments were averaged (see "Appendix"), and the averaged data were preprocessed in Filemaker Pro to identify genes with a mean minimum quality statistic (35) of 0.6 (scale 0–1) and mean intensity in the Cy5 or Cy3 channel of >500 units (scale 0–65,535). Genes were also retained if the mean Cy5 or Cy3 intensity in any one cell line exceeded 1000 units. To identify responsive genes (deviating in expression ratio), we filtered for genes showing a ratio > 1.5 fold, with a quality > 0.75 and intensity measurement > 1100. A 1.5-fold cutoff for expression ratio was calculated to be statistically significant ($P < 0.01$); average ratio variation from duplicated (approximately eight repeats/array) housekeeping clones within an array was 1.22 with no single experiment exceeding 1.5; average ratio variation for the same array feature within paired duplicates for the set of 42 duplicate experiments was 1.34; ratio variation between three self-self experiments was 1.44, 1.41, and 1.42. We arbitrarily chose 19 ratio measurements between 1.5 and 2 for Quantitative Reverse Transcription-PCR validation 19 of 19 validated the direction and 18 of 19 the magnitude of response (data available upon request). For genes with a 1.5-fold expression change and an average Cy5 or Cy3 intensity of <2250 units in any cell line, we increased the fold expression ratio stringency in this range to 2. Lastly, we omitted genes that displayed a Cy5 or Cy3 dye bias across >28 of the 42 experimental conditions.

Hierarchical Clustering. Data were analyzed using web-based resources available at the NIH.[5] Uncentered Pearson's correlation was used on log-transformed data, with induced genes indicated in red and repressed genes in green. Gray indicates data points with quality < 0.3 units and intensity (in both channels) < 300 units.

Statistical Comparison with ER Status and Metastasis Discriminator Genes from Tumor Expression Profiles. An association between our gene expression clusters and the ER status and patient prognosis discriminator genes reported by van't Veer *et al.* (15) was established using a χ^2 test. Because the number of discriminator genes present in some clusters was small, we estimated *P*s using a Monte Carlo procedure: 100,000 replicates were generated by random sampling from the set of all contingency tables with marginal data identical to the original data, and the probability to get a χ^2 larger than the original data was calculated. Once an overall association between clusters and ER status or prognosis genes was established, each cluster was separately analyzed for association with ER status or prognosis genes. The odds ratio of the odds for a gene in a cluster to be a discriminator gene to the same odds for a gene in all other clusters (2×2 table) was calculated using the conditional maximum likelihood estimate. *P*s for the odds ratios were calculated using Fisher's exact test.

GO Analysis. The GO (36) provides annotation for 60% of the clones in our experiments. From the directed acyclic graph structure of the GO, each node of annotation is coupled to overlying and underlying nodes via "has a" and "part of" relations. This implies that a clone mapped to any given node in the GO is also mapped to that node's parent nodes. As the GO provides a mapping from LocusLink identifiers[6] to GO nodes, we mapped each clone to a UniGene cluster, then used the LocusLink identifier associated with each UniGene cluster to assign each clone to GO nodes. We removed clone redundancy and different clones representing the same UniGene cluster (leaving one representative copy in the dataset for ontology analysis). We used reshuffling[7] to sort the list of expression patterns with respect to similarity. Briefly, this algorithm is based on a quality function, describing an interaction between the distance of any two expression patterns on the list of genes and the similarity of the patterns defined by Pearson's correlation. The algorithm results in a sorted gene list with the most correlated expression patterns adjacent. We analyzed the sorted lists using the GO by investigating if genes belonging to a GO node were associated with specific parts of the list. Briefly, we calculated the number of genes belonging to each GO node in a sliding window moving along the sorted list. For each GO node, we set the size of the sliding window such that we would on average expect four genes belonging to the node in each window for a randomly sorted list. Because each GO node had a different number of genes in the list, this means that the window size was set separately for each GO node. For each window and GO node, we plotted the number of genes belonging to the GO node divided by the expected number. Aligning these gene density plots with the sorted expression data provides for a way to associate expression patterns with specific GO nodes.

RESULTS AND DISCUSSION

Experimental Design and Global Changes in Gene Expression. Expression profiles from three breast cancer cell lines, MCF7, T-47D (both ER+), and MDA-MB-436 (ER−), were compared at time points (2, 8, and 24 h) after treatment with growth agonists and antagonists known to affect breast cancer cell proliferation. The 14 different combinations of cell line and drug treatment are listed in

[3] Internet address: http://www.ncbi.nlm.nih.gov/UniGene/.
[4] Internet address: http://research.nhgri.nih.gov/microarray/.
[5] Internet address: http://arrayanalysis.nih.gov/.
[6] Internet address: http://www.ncbi.nlm.nih.gov/LocusLink.
[7] Internet address: http://www.thep.lu.se/pub/Preprints/00/lu_tp_00_18.pdf.

Table 1 and were conducted in biological replicate. Cell line-specific variations in the proliferative response to each agent were measured to aid in subsequent biological interpretation of gene expression data (Fig. 1). The most potent growth inhibitor of MCF7 cells was ICI and atRA for T47D cells. Steroid hormones did not stimulate the growth of ER− MDA-MB-436 cells as expected. Eighty-four hybridizations were performed on microarray slides containing 13,824 cDNAs. Duplicate experiments were averaged using a quality weighted algorithm (see "Appendix"), resulting in 42 data points for each gene. We stringently filtered our data for quality, then identified genes that responded >1.5-fold in 2 or more of the 42 conditions (see "Materials and Methods"). A total of 1023 unique genes met these requirements. Numerical data for the 1023 responsive genes is provided in supplementary Table 1. Analysis of gene expression responsiveness across the entire dataset revealed a remarkable set of 47 genes that responded in six or more different cell line/treatment conditions (Fig. 2, *A* and *B*). A high proportion of these genes encode proteins known to be strongly associated with oncogenesis such as *MYC*, *ERBB2*, *CCND1*, *CD44*, and *ETS* family members. Five of these 47 genes are ESTs, which certainly warrant additional investigation. Global gene expression responses across this dataset are summarized in Fig. 2*C*. Every cell line/treatment resulted in both activation and repression of gene expression, with the number of responsive genes increasing with time, except for EGF and TPA treatments, which exhibited an early peak in responsiveness. The most dramatic response was in MCF7 cells treated with TPA, and the smallest response was to RU486 in MCF7 cells.

Hierarchical Clustering of Hormonally Regulated Genes. A total of 386 genes identified to be responsive in the 24 hormone-related experiments (see "Materials and Methods") was grouped by hierarchical clustering (Fig. 3, see also supplementary Fig. 1). atRA was included in this clustering to facilitate comparison of expression signatures between the agents that act on nuclear receptors. Each agent caused discrete but interrelated patterns of gene expression, including both induction and repression. Overall, we observed a reciprocal pattern of gene regulation in MCF7 cells treated with E2 and antagonists ICI and 4-OHT. Many of the E2-induced genes (Fig. 3, *i* and *iii*) have previously been reported to be up-regulated by E2 (19–21, 23–25). The antiestrogen effects of ICI are more profound than that of 4-OHT, consistent with previous studies (37, 38). The pattern of progestin stimulation in the two hormone-responsive cell lines displayed significant differences, in particular, a large cluster of genes specifically up-regulated in T47D by R5020 (Fig. 3, *vii*). This is not unexpected given the large amount of progesterone receptor expressed in T47D. Additionally, these cells express a high level of ER-β compared with MCF7 (39), and given the slight estrogenic effect of R5020 observed at 10^{-6} M (40), the T47D/R5020 expression profile may, in part, be mediated by estrogen receptors. The strong T47D/R5020 response is consistent with the higher degree of responsiveness of T47D to RU486 compared with MCF7 (Fig. 2*C*). The expression profile of MCF7 treated with E2 or R5020 appeared remarkably similar, although the response to R5020 was less pronounced. This observation is consistent with previously reported evidence of a weak estrogenic effect of R5020 on MCF7 cells and the previously observed abrogation of progestin-induced growth of MCF7 in the presence of antiestrogens (40, 41). Retinoic acid treatment resulted in a distinct pattern of gene expression, although this contains striking overlaps with ICI treatment (Fig. 3, *ii* and *iv*), illustrating common features in the transcriptional effects of these negative growth regulators.

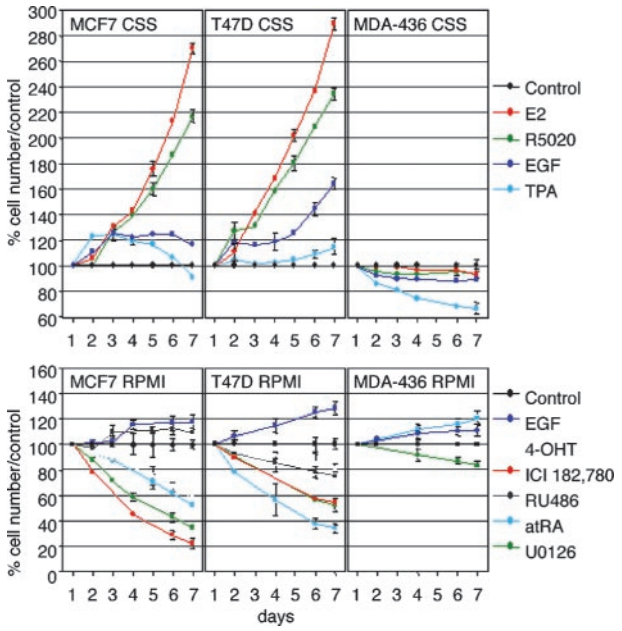

Fig. 1. Variations in proliferative response to growth agonists and antagonists. Cell growth rates after drug treatment (MTT assay) were plotted relative to untreated (control) cells (percentage). In the *top three graphs*, cell lines were treated in media devoid of hormones and peptide growth factors (CSS), and *bottom panels* show cell growth rates in complete medium (RPMI). Only ER+ cell lines responded to steroid agonists and antagonists as expected. *Error bars* indicate SE from assays conducted in triplicate.

Table 1 *Cell lines and drug treatments*[a]

Treatment	Final concentration	Growth medium	Cell lines		
			MCF7	T47-D	MDA-436
E2	10 nM	CSS	[a]		
ICI	100 nM	Complete	[a]		
4-OHT	100 nM	Complete	[a]		
R5020	1 μM	CSS	[a]	[a]	
RU486	1 μM	Complete	[a]	[a]	
atRA	1 μM	Complete	[a]		
EGF	25 μg/ml	CSS	[a]		[a]
U0126	10 μM	Complete	[a]		[a]
TPA	100 nM	CSS	[a]		[a]

[a] Represents a total of six microarray hybridizations conducted, two at each time point (2, 8, and 24 h).

CSS denotes media devoid of hormones and peptide growth factors (refer to "Materials and Methods").

Hierarchical Clustering of Genes Regulated in Kinase Signaling. Hierarchical clustering of expression changes in MCF7 and MDA-MB-436 cells treated with EGF to activate signaling of the MAPK cascade, U0126, a specific inhibitor of Mek1/2 kinase in this cascade, and phorbol ester TPA, which activates PKC signaling, is shown in Fig. 4*A* (see supplementary Fig. 2). Similar to the hormone data, we observed genes regulated in a reciprocal fashion between EGF and U0126 treatment, indicating these genes are likely to be regulated after activation of Mek1/2 kinase and downstream effectors. The magnitude of the response of MCF7 to TPA treatment was large and more pronounced than that of MDA-MB-436. This may reflect the differences in phorbol ester sensitivity and PKC isoform expression/activation between ER+ and ER− breast cancer cells (42–44). Many of the clusters in Fig. 4*A* indicate cell type-specific gene regulation (Fig. 4*A*, *i* and *ii*, responsive to EGF and TPA in MCF7, Fig. 4*A*, *iv* and *v*, responsive only in MDA-MB-436). We also observed a strong cluster of genes induced by TPA and EGF in both cell lines (Fig. 4*A*, *iii*). We observed a striking similarity in the pattern of gene expression with EGF and TPA in MCF7 (and similarly EGF and TPA in MDA-MB-436). As the pattern of EGF regulation is likely to denote a MAPK activation signature, the pattern similarity with TPA is consistent with reports describing PKC signaling to the MAPK axis (45, 46). Moreover, the profound induction of gene expression by

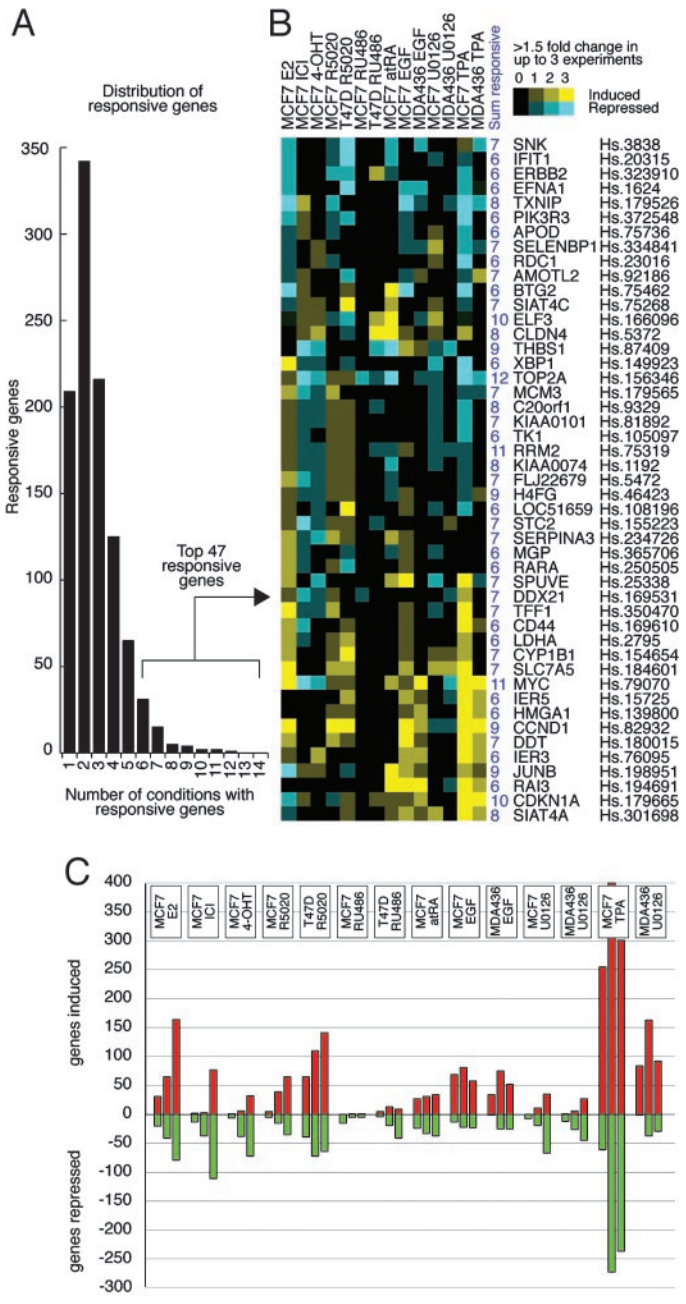

Fig. 2. Overview of responsive genes. *A*, distribution of genes identified to be responsive (see "Materials and Methods") in at least one time point in the panel of cell line/treatment conditions. Most genes responded in one to four conditions and a limited number responded in multiple conditions. *B*, forty-seven genes that responded in six or more different conditions in at least one time point are shown (response in zero, one, two, or three time points within a condition is indicated by increasing color brightness in the mosaic). Hierarchical clustering of this data were used to visualize the frequency of genes responsive across the 14 discrete conditions, as well as the shared and reciprocal patterns of response between conditions. For example, most genes induced by TPA are also induced by EGF. There are also strong reciprocal patterns of response between E2 and antiestrogen treatments. *C*, summary of the magnitude and direction of genes responsive in each of the 42 time points analyzed.

TPA in MCF7 suggested dramatically enhanced activation of MAPK by TPA. We examined activation of MAPK in MCF7 after EGF or TPA by immunoblotting (Fig. 4*B*). EGF-mediated MAPK activation peaked at 15 min without an increase in p44/42 MAPK protein, in agreement with previous data (47). TPA treatment of MCF7 cells resulted in prolonged phosphorylation of MAPK without a parallel increase in p44/42 MAPK protein level. A similar but delayed pattern of TPA-mediated MAPK phosphorylation was observed in MDA-MB-436 cells. Data consistent with growth arrest of TPA-treated MCF7 cells were a 6-fold increase in $p21^{WAF1/CIP1}$ expression by 2 h, a 4.5-fold decrease in ER expression by 24 h and significant changes in morphology (Fig. 4*C*). There are numerous studies discussing the role of MAPK overstimulation and PKC activation in breast cancer. The complex impact of growth factors on these signaling mechanisms (including phosphorylation of ER and associated coactivators, as well as the level of expression of ER itself; Refs. 28, 48, 49), highlights the interaction between these signaling mechanisms.

Hierarchical Clustering Analysis across All Conditions Reveals a Complex Pattern of Response to Growth Regulators. The power of gene clustering to define both distinct and overlapping patterns of gene expression associated with each drug is demonstrated when all experimental conditions are analyzed together (Fig. 5*A*, see supplementary Fig. 3). Immediately evident was a profound overlap in genes regulated by steroids and those regulated in the kinase signaling cascades. This is consistent with recent literature discussing the ability of E2 to stimulate cell growth via nonclassical and nonnuclear pathways, including direct interaction of membrane-associated ER and

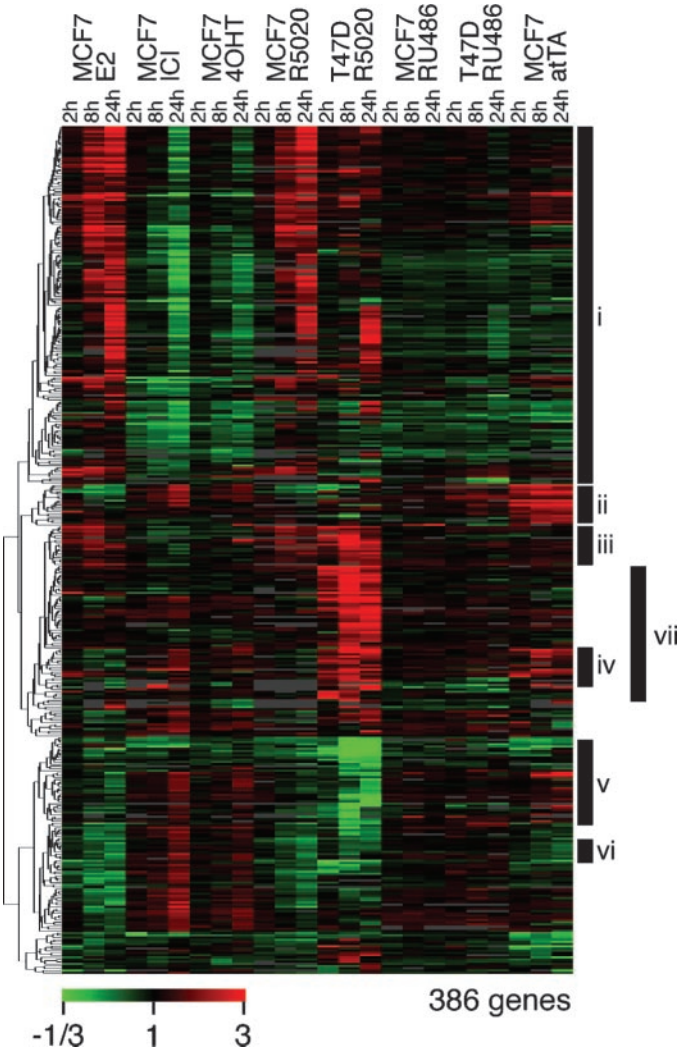

Fig. 3. Hierarchical clustering of hormonally regulated genes. A total of 386 genes was identified to be responsive in at least 2 of the 24 hormone-related experiments. See supplementary Fig. 1 for gene list. For each cell line/drug treatment, expression profiles for the 2, 8, and 24 h time points are plotted from left to right in the mosaic. Clusters i and iii, steroid hormone-induced genes, ii and iv, retinoic acid-induced genes, the majority of which are also induced by ICI treatment. v contains many IFN-inducible genes, and vi is a tight cluster of histone family members. Cluster vii represents genes strongly induced by R5020 in T47D cells.

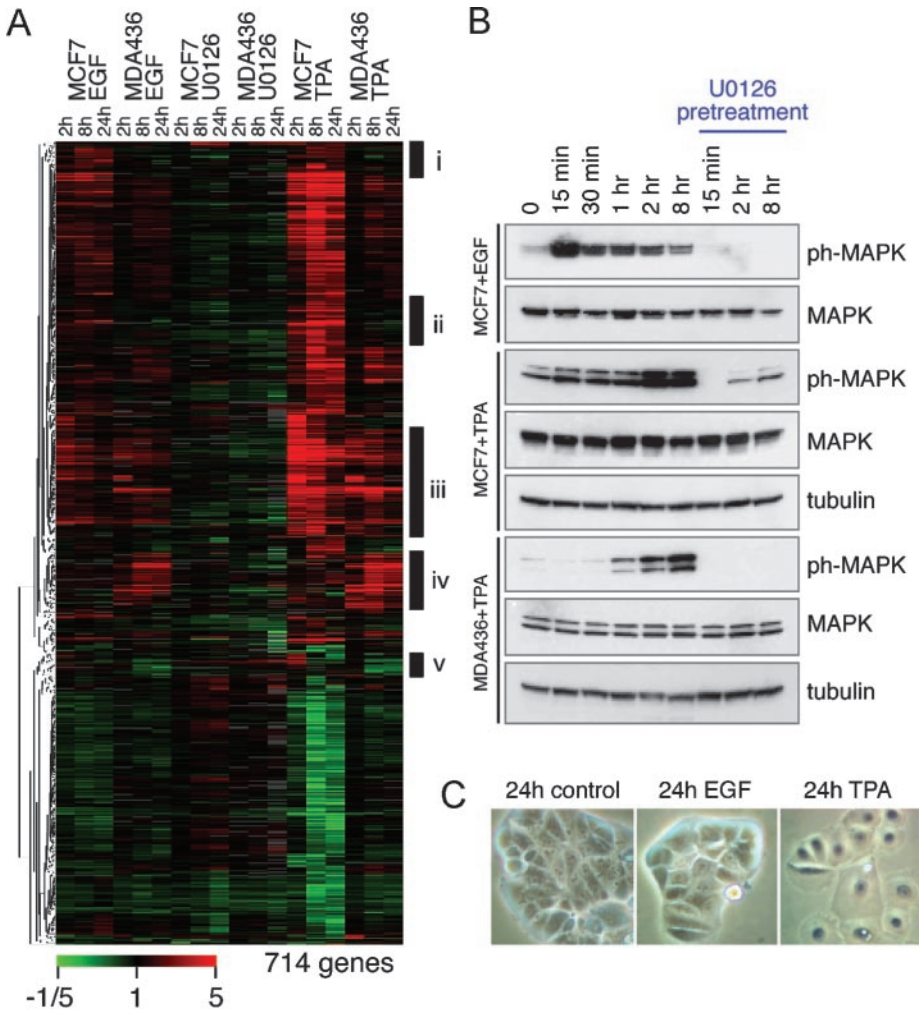

Fig. 4. Genes regulated in kinase signaling. *A*, hierarchical clustering dendrogram of 714 genes responsive in at least 2 of the 18 experimental conditions. See supplementary Fig. 2 for gene list. *B*, Western blot analysis of MAPK activation by EGF and TPA. Levels of phospho-p44/42 MAPK and p44/42 MAPK were measured in parallel from whole cell lysates. Where indicated, 1 μM U0126 Mek1/2 inhibitor was added to cells 30 min before EGF or TPA treatment to block MAPK phosphorylation. *c*, morphology of MCF7 cells after 24 h EGF, TPA, or vehicle control treatment. TPA rapidly (even by 1 h, data not shown) induces a cytostatic morphology indicative of growth arrest, not seen with EGF-treated or control cells.

Src, E2 action via G protein-coupled receptors, ERBB2, as well as activation of adenylate-cyclase and protein kinase A/PKC (47, 50–54). Fig. 5*A* shows a number of very distinct clusters. Cluster vi harbors genes strongly induced by E2 and strongly repressed by the antiestrogens and TPA. Sixty percent of the genes in this cluster are associated with mitosis, DNA synthesis, RNA processing, cell cycle regulation, including a number of known S-phase targets of phospho-RB, including *DHFR*, *TK1*, *CDC2*, and *CCNA*. Moreover, regulation of $p21^{WAF1/CIP1}$ expression (E2 repressed and strongly TPA induced) is consistent with regulation of these genes. In dramatic contrast to Fig. 5*A* cluster vi are clusters ii and iii, which also contain genes highly induced by E2, but unlike cluster vi, these genes are induced by EGF and TPA and repressed by U0126 and thus represent an important set of genes involved in E2-mediated MAPK signaling, a pathway critical for cell migration and tumor progression. This separation of the bulk of E2-induced genes into distinct clusters illustrates the necessity of studying ER-mediated signaling in the context of other signaling pathways. A number of the cell type-specific clusters observed in Figs. 3 and 4*A* are maintained in Fig. 5*A*. For example, Fig. 5*A* cluster iv, a group of 23 genes induced by EGF and TPA only in MDA-436 cells, contains a striking number of biologically related genes, including four modulators of tumor growth factor β member signaling (*FST*, *CKTSF1B1*, *SMURF2*, and *TSC22*) and five immune, stress, and inflammatory response genes (*CSF3*, *IL1B*, *IL6*, *CCL3*, and *CXCL1*).

Correlation of ER Status and Metastatic Disease Discriminator Genes from Tumor Expression Profiles with Growth Factor-Regulated Genes. Because of the important clinical implications of ER status in breast cancer, we interrogated our clustered genes in Fig. 5*A* for possible correlations with breast tumor gene expression signatures that discriminate ER+ from ER− tumors and separately for genes associated with metastatic disease. We used the recent data of van't Veer *et al.* (15) because the large number of genes included on their microarrays was likely to provide a good overlap with our gene set. First, of their 2460 ER status discriminator genes, we associated 1720 to a UniGene cluster (build 154), and 1365 of these were present on our arrays. Comparing these 1365 genes to the 1023 responsive genes included in Fig. 5*A*, we found 158 clones in common (54 were more highly expressed in ER+ tumors (ER+ discriminators) and 104 in ER− tumors (ER− discriminators), according to van't Veer *et al.* (15). This suggests that the majority of tumor ER status genes are not associated with the regulatory events observed in this *in vitro* study. We mapped the positions of the 158 discriminators with respect to the 44 clusters in Fig. 5*A* (determined from the hierarchical gene tree, refer to supplementary Fig. 3) and, established using a χ^2 test (see "Materials and Methods"), that these ER discriminators are not randomly distributed among the clusters (for ER+ discriminators, $P < 0.0003$, and for ER− discriminators, $P < 0.0001$; see supplementary Fig. 3 for gene comparison). Odds ratios calculated for each of the 44 clusters indicated that four clusters, iv–vii had statistically

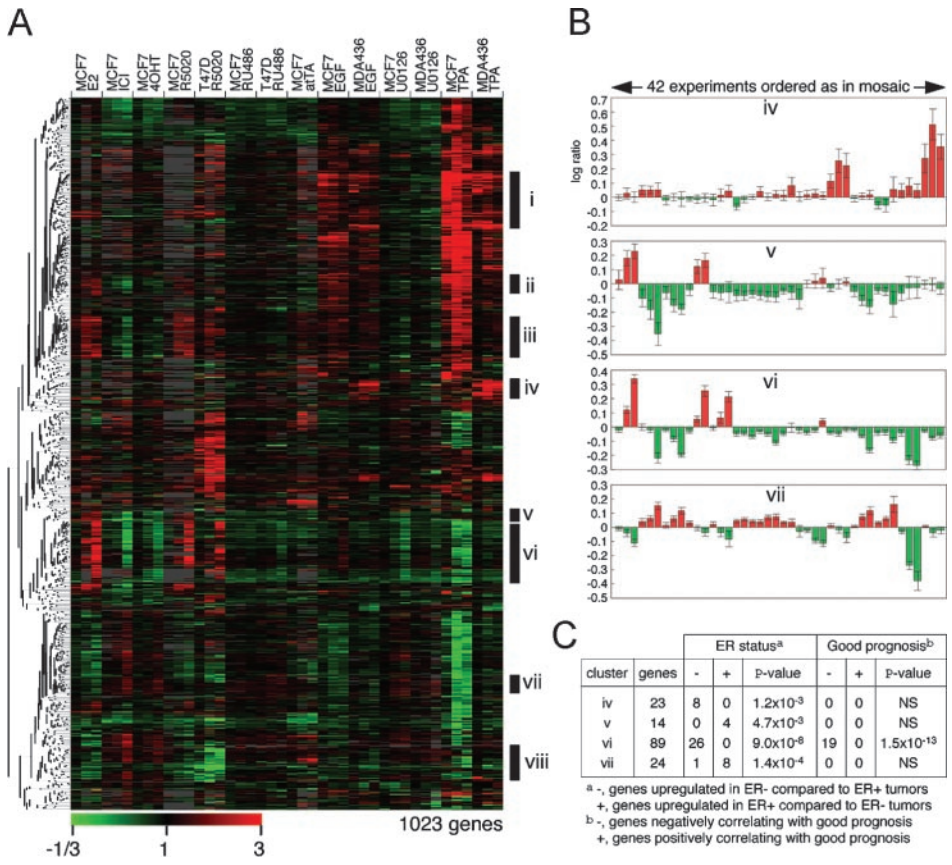

C

		ER status[a]			Good prognosis[b]		
cluster	genes	-	+	p-value	-	+	p-value
iv	23	8	0	1.2×10^{-3}	0	0	NS
v	14	0	4	4.7×10^{-3}	0	0	NS
vi	89	26	0	9.0×10^{-8}	19	0	1.5×10^{-13}
vii	24	1	8	1.4×10^{-4}	0	0	NS

[a] -, genes upregulated in ER- compared to ER+ tumors
+, genes upregulated in ER+ compared to ER- tumors
[b] -, genes negatively correlating with good prognosis
+, genes positively correlating with good prognosis

Fig. 5. Hierarchical clustering across all conditions and comparison of expression clusters with ER status or disease outcome discriminator genes from tumor expression profiles. *A*, hierarchical clustering dendrogram of 1023 genes identified to be responsive in at least 2 of the 42 experiments. See supplementary Fig. 3 for gene list. Clusters i–viii are discussed in the text. *B*, the four plots aid in visualizing the average expression values (log transformed) within clusters iv–vii for all 42 experiments. *Error bars* are $2\sigma/\sqrt{n}$ (95% confidence interval). *c*, a significant association between the 1023 responsive genes shown in *a* and two sets of genes reported by van't Veer *et al.* (15) as discriminatory for either tumor ER-status or for patient prognosis was established. Clusters iv–vii showed statistically higher numbers of discriminator genes than expected ($P < 0.01$). NS, not statistically significant. For comparative lists of genes in these clusters, refer to supplementary Fig. 3.

more ER discriminator genes than expected by random chance ($P < 0.01$), as summarized in Fig. 5*C*. The average log expression ratios in each experiment for clusters iv–vii are shown in Fig. 5*B*. Fig. 5*A*, *ii*, showed a weaker correlation ($P = 0.015$) with ER− status genes. The highest correlation for this comparison was observed for Fig. 5A, cluster vi ($P = 9.0 \times 10^{-8}$), which contains many steroid hormone-induced genes, and is the proliferation cluster discussed in the previous section. Remarkably, 30% of the genes in this cluster are ER discriminators, and all 26 of these genes are ER− discriminators. This dramatic correlation may, in part, reflect the higher flow cytometric S-phase fraction observed in ER− breast tumors (55), and the high proportion of S phase, mitosis, and cell cycle-related genes in this cluster. Conversely to cluster Fig. 5*A*, vi, the estrogen-induced genes in cluster v contain four ER+ status genes, *ASAHI*, *NRIP1*, *MYB*, and *XBP1*, a larger number than expected by chance ($P = 4.7 \times 10^{-3}$). This cluster interestingly lacks T47D progestin-induced genes and lacks genes down-regulated by TPA (compare Fig. 5*B* clusters v and vi). Importantly, Fig. 5*A*, cluster iii, the second large cluster of strongly E2-induced genes, does not correlate at all with ER discriminator genes. Lastly, Fig. 5*A*, cluster iv showed a significant correlation ($P = 0.0012$) with genes discriminatory for the more aggressive ER− tumor type. Remarkably, of the eight ER discriminators in this cluster (*CCL3*, *CXCL1*, *IL1B*, *IL6*, *CALB2*, *CTSL*, *ALDH1A3*, and *VIM*), four are known to be involved in acute inflammatory processes (chemokines *CCL3* and *CXCL1* and interleukins *IL1B* and *IL6*). *VIM* has previously been reported as a predictor of more aggressive/invasive breast cell behavior (56).

Similar to the comparison with the ER discriminators, we conducted a comparison of our 1023 drug-responsive genes with the 231 genes identified by van't Veer *et al.* (15) as significantly associated with disease outcome. One-hundred fifty-two of the 231 genes were present on our arrays (107 with higher expression in metastatic tumors and 45 in nonmetastatic tumors). Forty-one of these 152 discriminators were present in our set of 1023 drug-responsive genes (see supplementary Fig. 3 for gene comparison). Using the χ^2 test, we established that these genes were not randomly distributed among our clusters (metastatic, $P < 0.0005$; nonmetastatic, $P < 0.05$). Remarkably, 19 of these 41 prognosis predictors are present in cluster vi, and all 19 were metastatic indicators [having higher expression in poor prognosis samples as compared with good prognosis samples ($P = 1.5 \times 10^{-13}$; Ref. 15)]. This is consistent with the known importance of S-phase fraction in determining patient prognosis (57). Of the 89 genes in Fig. 5 cluster vi, 37 are either ER− discriminators or indicators of poor prognosis (eight genes are discriminatory for both), which is consistent with the proliferation signature defining this cluster.

GO Mapping of Expression Profiles Identifies Functional Responses to Drug Treatments. Mapping of genes to GO nodes is a powerful functional genomics tool suited to the analysis of microarray data because one can discover whether related groups of genes from expression clustering share significant functional annotation in the GO database. Our data were analyzed with respect to the ontology provided by the GO Consortium (36). We have developed a novel method to identify the most significant GO nodes associated with gene expression patterns in individual or combinations of drug treatment profiles. This method involves first re-sorting gene expression profiles of interest using a reshuffling algorithm (see "Materials and Methods"), which reorders expression patterns such that the most correlated patterns become adjacent. This method is especially suited to extract the structure of smoothly varying data patterns typical of time course analyses. As a result, we observe a time course-like dimensionality along the reordered genes that cannot easily be achieved using most existing clustering methods. GO terms harboring dense numbers of genes with shared annotations are then identified

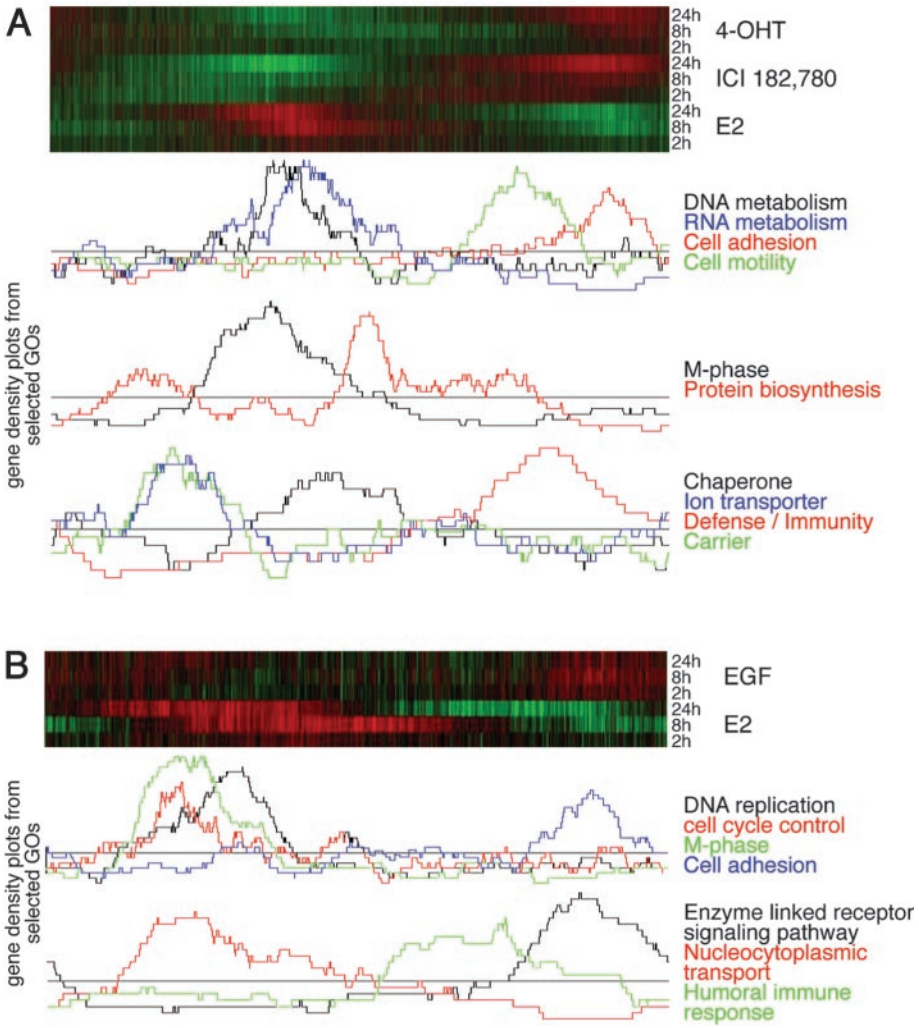

Fig. 6. GO mapping of expression profile data. E2 and E2 antagonist expression data were filtered for minimum quality requirements and reshuffled as described in the "Materials and Methods." The result is shown in the *top red/green plot*, with experimental conditions ordered vertically and reshuffled genes shown horizontally. The 4310 genes included in the reshuffling were mapped to the GO database (see "Materials and Methods"), and nodes containing dense numbers of genes were individually examined and plotted if they showed visual correlation with the strongest peaks in the reshuffling plot. *B*, EGF compared with E2 data (4825 genes) were reshuffled relative to each other, and gene density plots were generated as in *A*. For complete lists of genes under each GO peak, refer to supplementary Table 1.

and positionally plotted relative to the peaks in gene expression changes in the reshuffling plot (see "Materials and Methods"). We present two examples using this method: first, comparing E2 and E2 antagonist data (Fig. 6*A*); and second, MCF7/E2 with MCF7/EGF data (Fig. 6*B*). Fig. 6*A* shows genes regulated by E2 and antiestrogens in MCF7. Using reshuffling and GO analysis, we identified distinct biological responses in this data, including a strong signal related to regulation of DNA and RNA metabolism and cell cycle genes, as well as cell motility and adhesion genes. Similarly, in Fig. 6*B*, comparison of the GO peaks characterizing the MCF7 E2 and EGF responses reveals differences between these two mitogens. For example, both ligands lead to striking GO signals for receptor signaling and for adhesion-related genes, but these genes were regulated in opposite directions by these two treatments. These examples demonstrate the power of the controlled vocabulary of the GO database to facilitate automated extraction of potentially useful biological information from expression data. These results can then be used to generate hypotheses to guide additional mechanistic studies of the distinct and overlapping pathways associated with various drug treatments.

In conclusion, this study provides a detailed analysis of genes that are induced or repressed by regulators of breast cancer cell growth in three breast cancer cell lines. By developing a database of gene regulation across a broad set of conditions, we identified a complex pattern of cell type and drug-specific responses in this dataset. Most strikingly, we report large regions of overlap in the pattern of genes regulated by steroid hormones, EGF, and TPA. The separation of E2-inducible genes into two or three groups, either positively or negatively regulated by TPA particularly illustrates the power of this approach. Although the interrelationships of these important signaling pathways have been discussed in recent literature, our data provides a novel overview of the relationship between the genes regulated by these signaling networks. This data also highlights inherent pharmacological differences and the overall impact at the gene expression level of clinically relevant agents. The observation of functionally related groups of genes in our expression clusters and GO analysis allows the identification of distinct biological pathways regulated by the agents used and provides the basis for future mechanistic studies. By comparing our *in vitro* gene expression data with data from tumor specimens (15), we observed that the majority of genes regulated in cell culture do not predict ER status in tumors. We conclude that these genes more likely reflect differences in the underlying histogenesis and mechanisms of disease progression in ER+ and ER− tumors rather than the impact of hormone signaling. Interestingly, we found that a larger proportion (41 of 152) of the prognosis indicators described by van't Veer *et al.* (15) are responsive to drug treatment in our dataset. We have established a connection between several gene clusters regulated in cell culture and genes that discriminate ER status and disease outcome in clinical specimens. These observations provide an opportunity to investigate these clusters for common mechanisms, which may be responsible for their coregulation in tumors.

Our data provides a number of additional opportunities for future studies. Many of the regulated genes, including some very responsive

genes (Fig. 2*B*), are ESTs. Investigation of these genes is likely to identify biochemical pathways relevant to the growth and differentiation of breast cancer cells. GO mapping has identified regulation in a number of functional categories, including cell adhesion and transport molecules, which have not been previously recognized as candidate targets of signal transduction pathways in breast cancer. It will be of considerable interest to examine the group of regulated genes we have identified for the presence of regulatory elements, which may account for their behavior. Finally, it will be possible to extend the comparison of our data with other clinical subsets such as hormone refractory ER+ tumors.

ACKNOWLEDGMENTS

We thank Dr. Abdel Elkahloun for production of cDNA microarray slides and Dr. Seungchan Kim for assistance with graphical output. We also thank Dr. David Azorsa and Dr. Ashani Weeraratna for help with Western blot analyses, Thomas Breslin for help regarding the GO, and Dr. Michael Bittner for his expertise and guidance in all aspects of this study.

APPENDIX

Cross-Array Normalization and Ratio Averaging. For a set of replicated experiments where RNA from the same test sample was replicated and hybridized, with the same reference RNA, to multiple arrays, we prefer to average expression ratios to reduce the noise level, as well as maintaining the characteristics of independence when compared with the other samples. Notice that the array-array variation may come from multiple sources such as print-batch variation and hybridization noises; we design the averaging process in two steps: cross-array normalization and weighted ratio averaging.

Cross-Array Normalization. Cross-array normalization is based on the fact that reference channel and test sample channel from replicated array are from the same RNA source, respectively. Therefore, beside the requirement that two channels within each array shall be correlated (which is the theoretical base of normalization relative to the reference channel for all experiments), we additionally constrain that for any two replicate experiments, the intensities of test sample channels, as well as intensities from reference channels, shall be correlated, with some level of interarray noises. Assume there are n replicated arrays for one test RNA, and let $r_{i,n}$ and $g_{i,n}$ denote the logarithm-transformed intensities from ith gene of test sample and reference sample in nth replication, respectively. When $r_{i,n}$ and g_i are correlated to some extent, the parameters (a_n and b_n) in the following regression are meaningful.

$$g_{i,n} = a_n r_{i,n} + b_n \tag{1}$$

In standard normalization procedure, we would like to find a set of normalization parameters (conversion parameters), $\{\alpha_n, \beta_n\}$ and

$$\begin{cases} r_{i,n} \leftarrow \alpha_{1,n} r_{i,n} + \beta_{1,n} \\ g_{i,n} \leftarrow \alpha_{2,n} g_{i,n} + \beta_{2,n} \end{cases} \quad \text{for all genes } i, \tag{2}$$

such that a_n will be 1 (or $\log a_n = 0$) and b_n will be 0. In cross-array normalization, we extend Eqs. 1 and 2 as follows:

$$y_{i,m,n} = a_{m,n} x_{i,m,n} + b_{m,n} \tag{3a}$$

where

$$x_{i,m,n} = \begin{cases} \alpha_{1,m} r_{i,m} + \beta_{1,m} & \text{if } m \le n \\ \alpha_{2,m} g_{i,m} + \beta_{2,m} & \text{if } m > n \end{cases},$$

$$\text{and } y_{i,m,n} = \begin{cases} \alpha_{1,n} r_{i,n} + \beta_{1,n} & \text{if } m < n \\ \alpha_{2,n} g_{i,n} + \beta_{2,n} & \text{if } m \ge n \end{cases} \tag{3b}$$

Clearly from Eq. 3b, the multiple normalization procedures were carried out between same channel across arrays, except for the case when $m = n$, in which regression will be performed between two channels within the same array. The cross-array normalization is achieved by minimizing,

$$\min_{\text{for all } \{\alpha,\beta\}} \{\sum_{m=1}^{N} \sum_{n=1}^{N} w_{m,n} |\log \alpha_{m,n}| + \sum_{m=1}^{N} \sum_{n=1}^{N} \dot{v}_{m,n} |b_{m,n}|) \tag{4}$$

where $w_{m,n}$ and $v_{m,n}$ are the weight for each corresponding regression parameter. In our cross-array normalization, we let $w_{m,n} = v_{m,n} = 2$ if $m = n$, otherwise $w_{m,n} = v_{m,n} = 1$. By using this weighting scheme, we enforce that the standard normalization to be more accurate (gene expression levels from each channel are correlated along 45 line) before cross-array normalization.

Weighted Ratio Averaging. After cross-array normalization in which ratios from all genes are corrected according to the normalization parameters given in Eq. 2, the weighted average expression ratio for ith gene, t_i, and its corresponding quality measure q_i, are

$$t_i = \begin{cases} \sum_{i=1}^{N} t_{i,m} w_{i,m} / \sum_{i=1}^{N} w_{i,m}, & \text{if } \sum_{i=1}^{N} w_{i,m} \neq 0 \\ \frac{1}{N} \sum_{i=1}^{N} t_{i,m}, & \textit{otherwise} \end{cases} \tag{5a}$$

$$q_i = \sum_{i=1}^{N} q_{i,m}^2 v_{i,m} / \sum_{i=1}^{N} v_{i,m} \tag{5b}$$

where $t_{i,m}$ is the logarithm-transformed expression ratio of ith gene in mth replication. $w_{i,m}$ is the weight of ith gene in mth replication, which is determined as follows:

$$w_{i,m} = q_{i,m}^2 \cdot [(r_{i,m} + g_{i,m})/2] \tag{6a}$$

$$v_{i,m} = [(r_{i,m} + g_{i,m})/2] \tag{9}$$

where $q_{i,m}$ is the measurement quality of ith gene in mth replication, and $(r_{i,m} + g_{i,m})/2$ is the average intensity of ith gene in mth replication. Eq. 6a is chosen because we need to weigh less for lower quality genes, and we need to put more weight for ratios with higher intensities. If all weights are zeroes, Eq. 5a reduces down to a simple average without any weights. The same procedure can be applied to intensities instead of ratio.

REFERENCES

1. Salh, B., Marotta, A., Matthewson, C., Ahluwalia, M., Flint, J., Owen, D., and Pelech, S. Investigation of the Mek-MAP kinase-Rsk pathway in human breast cancer. Anticancer Res, *19:* 731–740, 1999.
2. Mueller, H., Flury, N., Eppenberger-Castori, S., Kueng, W., David, F., and Eppenberger, U. Potential prognostic value of mitogen-activated protein kinase activity for disease-free survival of primary breast cancer patients. Int. J. Cancer, *89:* 384–388, 2000.
3. Darbon, J. M., Valette, A., and Bayard, F. Phorbol esters inhibit the proliferation of MCF-7 cells. Possible implication of protein kinase C. Biochem. Pharmacol., *35:* 2683–2686, 1986.
4. de Vente, J. E., Kukoly, C. A., Bryant, W. O., Posekany, K. J., Chen, J., Fletcher, D. J., Parker, P. J., Pettit, G. J., Lozano, G., Cook, P. P., *et al.* Phorbol esters induce death in MCF-7 breast cancer cells with altered expression of protein kinase C isoforms. Role for p53-independent induction of gadd-45 in initiating death. J. Clin. Investig., *96:* 1874–1886, 1995.
5. Lee, C. S., Koga, M., and Sutherland, R. L. Modulation of estrogen receptor and epidermal growth factor receptor mRNAs by phorbol ester in MCF 7 breast cancer cells. Biochem. Biophys. Res. Commun., *162:* 415–421, 1989.
6. Saceda, M., Knabbe, C., Dickson, R. B., Lippman, M. E., Bronzert, D., Lindsey, R. K., Gottardis, M. M., and Martin, M. B. Post-transcriptional destabilization of estrogen receptor mRNA in MCF-7 cells by 12-*O*-tetradecanoylphorbol-13-acetate. J. Biol. Chem., *266:* 17809–17814, 1991.
7. Tzukerman, M., Zhang, X. K., and Pfahl, M. Inhibition of estrogen receptor activity by the tumor promoter 12-*O*- tetradeconylphorbol-13-acetate: a molecular analysis. Mol. Endocrinol., *5:* 1983–1992, 1991.
8. Gudas, L. J. Retinoids, retinoid-responsive genes, cell differentiation, and cancer. Cell Growth Differ., *3:* 655–662, 1992.
9. Hong, W. K., and Sporn, M. B. Recent advances in chemoprevention of cancer. Science (Wash. DC), *278:* 1073–1077, 1997.
10. Budd, G. T., Adamson, P. C., Gupta, M., Homayoun, P., Sandstrom, S. K., Murphy, R. F., McLain, D., Tuason, L., Peereboom, D., Bukowski, R. M., and Ganapathi, R. Phase I/II trial of all-*trans*-retinoic acid and tamoxifen in patients with advanced breast cancer. Clin Cancer Res., *4:* 635–642, 1998.
11. Perou, C. M., Jeffrey, S. S., van de Rijn, M., Rees, C. A., Eisen, M. B., Ross, D. T., Pergamenschikov, A., Williams, C. F., Zhu, S. X., Lee, J. C., Lashkari, D., Shalon, D., Brown, P. O., and Botstein, D. Distinctive gene expression patterns in human mammary epithelial cells and breast cancers. Proc. Natl. Acad. Sci. USA, *96:* 9212–9217, 1999.

12. Perou, C. M., Sorlie, T., Eisen, M. B., van de Rijn, M., Jeffrey, S. S., Rees, C. A., Pollack, J. R., Ross, D. T., Johnsen, H., Akslen, L. A., Fluge, O., Pergamenschikov, A., Williams, C., Zhu, S. X., Lonning, P. E., Borresen-Dale, A. L., Brown, P. O., and Botstein, D. Molecular portraits of human breast tumours. Nature (Lond.), *406:* 747–752, 2000.
13. Gruvberger, S., Ringner, M., Chen, Y., Panavally, S., Saal, L. H., Borg, A., Ferno, M., Peterson, C., and Meltzer, P. S. Estrogen receptor status in breast cancer is associated with remarkably distinct gene expression patterns. Cancer Res., *61:* 5979–5984, 2001.
14. Sorlie, T., Perou, C. M., Tibshirani, R., Aas, T., Geisler, S., Johnsen, H., Hastie, T., Eisen, M. B., van de Rijn, M., Jeffrey, S. S., Thorsen, T., Quist, H., Matese, J. C., Brown, P. O., Botstein, D., Eystein Lonning, P., and Borresen-Dale, A. L. Gene expression patterns of breast carcinomas distinguish tumor subclasses with clinical implications. Proc. Natl. Acad. Sci. USA, *98:* 10869–10874, 2001.
15. van't Veer, L. J., Dai, H., van de Vijver, M. J., He, Y. D., Hart, A. A., Mao, M., Peterse, H. L., van der Kooy, K., Marton, M. J., Witteveen, A. T., Schreiber, G. J., Kerkhoven, R. M., Roberts, C., Linsley, P. S., Bernards, R., and Friend, S. H. Gene expression profiling predicts clinical outcome of breast cancer. Nature (Lond.), *415:* 530–536, 2002.
16. van de Vijver, M. J., He, Y. D., van't Veer, L. J., Dai, H., Hart, A. A., Voskuil, D. W., Schreiber, G. J., Peterse, J. L., Roberts, C., Marton, M. J., Parrish, M., Atsma, D., Witteveen, A., Glas, A., Delahaye, L., van der Velde, T., Bartelink, H., Rodenhuis, S., Rutgers, E. T., Friend, S. H., and Bernards, R. A gene-expression signature as a predictor of survival in breast cancer. N. Engl. J. Med., *347:* 1999–2009, 2002.
17. West, M., Blanchette, C., Dressman, H., Huang, E., Ishida, S., Spang, R., Zuzan, H., Olson, J. A., Jr., Marks, J. R., and Nevins, J. R. Predicting the clinical status of human breast cancer by using gene expression profiles. Proc. Natl. Acad. Sci. USA, *98:* 11462–11467, 2001.
18. Ross, D. T., Scherf, U., Eisen, M. B., Perou, C. M., Rees, C., Spellman, P., Iyer, V., Jeffrey, S. S., Van de Rijn, M., Waltham, M., Pergamenschikov, A., Lee, J. C., Lashkari, D., Shalon, D., Myers, T. G., Weinstein, J. N., Botstein, D., and Brown, P. O. Systematic variation in gene expression patterns in human cancer cell lines. Nat. Genet., *24:* 227–235, 2000.
19. Charpentier, A. H., Bednarek, A. K., Daniel, R. L., Hawkins, K. A., Laflin, K. J., Gaddis, S., MacLeod, M. C., and Aldaz, C. M. Effects of estrogen on global gene expression: identification of novel targets of estrogen action. Cancer Res., *60:* 5977–5983, 2000.
20. Soulez, M., and Parker, M. G. Identification of novel oestrogen receptor target genes in human ZR75-1 breast cancer cells by expression profiling. J. Mol. Endocrinol., *27:* 259–274, 2001.
21. Lobenhofer, E. K., Bennett, L., Cable, P. L., Li, L., Bushel, P. R., and Afshari, C. A. Regulation of DNA replication fork genes by 17β-estradiol. Mol. Endocrinol., *16:* 1215–1229, 2002.
22. Wan, Y., and Nordeen, S. K. Overlapping but distinct gene regulation profiles by glucocorticoids and progestins in human breast cancer cells. Mol. Endocrinol., *16:* 1204–1214, 2002.
23. Seth, P., Krop, I., Porter, D., and Polyak, K. Novel estrogen and tamoxifen induced genes identified by SAGE (Serial Analysis of Gene Expression). Oncogene, *21:* 836–843, 2002.
24. Inoue, A., Yoshida, N., Omoto, Y., Oguchi, S., Yamori, T., Kiyama, R., and Hayashi, S. Development of cDNA microarray for expression profiling of estrogen-responsive genes. J. Mol. Endocrinol., *29:* 175–192, 2002.
25. Levenson, A. S., Kliakhandler, I. L., Svoboda, K. M., Pease, K. M., Kaiser, S. A., Ward, J. E., III, and Jordan, V. C. Molecular classification of selective oestrogen receptor modulators on the basis of gene expression profiles of breast cancer cells expressing oestrogen receptor alpha. Br. J. Cancer, *87:* 449–456, 2002.
26. Migliaccio, A., Di Domenico, M., Castoria, G., de Falco, A., Bontempo, P., Nola, E., and Auricchio, F. Tyrosine kinase/p21ras/MAP-kinase pathway activation by estradiol-receptor complex in MCF-7 cells. EMBO J., *15:* 1292–1300, 1996.
27. Improta-Brears, T., Whorton, A. R., Codazzi, F., York, J. D., Meyer, T., and McDonnell, D. P. Estrogen-induced activation of mitogen-activated protein kinase requires mobilization of intracellular calcium. Proc. Natl. Acad. Sci. USA, *96:* 4686–4691, 1999.
28. Font de Mora, J., and Brown, M. AIB1 is a conduit for kinase-mediated growth factor signaling to the estrogen receptor. Mol. Cell. Biol., *20:* 5041–5047, 2000.
29. Filardo, E. J., Quinn, J. A., Bland, K. I., and Frackelton, A. R., Jr. Estrogen-induced activation of Erk-1 and Erk-2 requires the G protein-coupled receptor homolog, GPR30, and occurs via *trans*-activation of the epidermal growth factor receptor through release of HB-EGF. Mol. Endocrinol., *14:* 1649–1660, 2000.
30. Azorsa, D. O., Cunliffe, H. E., and Meltzer, P. S. Association of steroid receptor coactivator AIB1 with estrogen receptor-α in breast cancer cells. Breast Cancer Res. Treat, *70:* 89–101, 2001.
31. Khan, J., Simon, R., Bittner, M., Chen, Y., Leighton, S. B., Pohida, T., Smith, P. D., Jiang, Y., Gooden, G. C., Trent, J. M., and Meltzer, P. S. Gene expression profiling of alveolar rhabdomyosarcoma with cDNA microarrays. Cancer Res., *58:* 5009–5013, 1998.
32. DeRisi, J., Penland, L., Brown, P. O., Bittner, M. L., Meltzer, P. S., Ray, M., Chen, Y., Su, Y. A., and Trent, J. M. Use of a cDNA microarray to analyse gene expression patterns in human cancer. Nat. Genet., *14:* 457–460, 1996.
33. Khan, J., Bittner, M. L., Chen, Y., Meltzer, P. S., and Trent, J. M. DNA microarray technology: the anticipated impact on the study of human disease. Biochim. Biophys. Acta, *1423:* M17–M28, 1999.
34. Chen, Y., Dougherty, E. R., and Bittner, M. L. Ratio-based decisions and the quantitative analysis of cDNA microarray images. J. Biomed. Optics, *2:* 364–374, 1997.
35. Chen, Y., Kamat, V., Dougherty, E. R., Bittner, M. L., Meltzer, P. S., and Trent, J. M. Ratio statistics of gene expression levels and applications to microarray data analysis. Bioinformatics, *18:* 1207–1215, 2002.
36. Ashburner, M., Ball, C. A., Blake, J. A., Botstein, D., Butler, H., Cherry, J. M., Davis, A. P., Dolinski, K., Dwight, S. S., Eppig, J. T., Harris, M. A., Hill, D. P., Issel-Tarver, L., Kasarskis, A., Lewis, S., Matese, J. C., Richardson, J. E., Ringwald, M., Rubin, G. M., and Sherlock, G. Gene ontology: tool for the unification of biology. The Gene Ontology Consortium. Nat. Genet., *25:* 25–29, 2000.
37. Diel, P., Smolnikar, K., and Michna, H. The pure antiestrogen ICI 182780 is more effective in the induction of apoptosis and down-regulation of BCL-2 than tamoxifen in MCF-7 cells. Breast Cancer Res. Treat, *58:* 87–97, 1999.
38. Bundred, N. J., Anderson, E., Nicholson, R. I., Dowsett, M., Dixon, M., and Robertson, J. F. Fulvestrant, an estrogen receptor down-regulator, reduces cell turnover index more effectively than tamoxifen. Anticancer Res., *22:* 2317–2319, 2002.
39. Vladusic, E. A., Hornby, A. E., Guerra-Vladusic, F. K., Lakins, J., and Lupu, R. Expression and regulation of estrogen receptor β in human breast tumors and cell lines. Oncol Rep., *7:* 157–167, 2000.
40. Jeng, M. H., Parker, C. J., and Jordan, V. C. Estrogenic potential of progestins in oral contraceptives to stimulate human breast cancer cell proliferation. Cancer Res., *52:* 6539–6546, 1992.
41. Schoonen, W. G., Joosten, J. W., and Kloosterboer, H. J. Effects of two classes of progestagens, pregnane and 19-nortestosterone derivatives, on cell growth of human breast tumor cells: I. MCF-7 cell lines. J Steroid Biochem Mol Biol, *55:* 423–437, 1995.
42. Fabbro, D., Regazzi, R., Costa, S. D., Borner, C., and Eppenberger, U. Protein kinase C desensitization by phorbol esters and its impact on growth of human breast cancer cells. Biochem. Biophys. Res. Commun., *135:* 65–73, 1986.
43. Nutt, J. E., Harris, A. L., and Lunec, J. Phorbol ester and bryostatin effects on growth and the expression of oestrogen responsive and *TGF-β1* genes in breast tumour cells. Br. J. Cancer, *64:* 671–676, 1991.
44. Shanmugam, M., Krett, N. L., Maizels, E. T., Murad, F. M., Rosen, S. T., and Hunzicker-Dunn, M. A role for protein kinase C δ in the differential sensitivity of MCF-7 and MDA-MB 231 human breast cancer cells to phorbol ester-induced growth arrest and p21(WAFI/CIP1) induction. Cancer Lett., *172:* 43–53, 2001.
45. Ueda, Y., Hirai, S., Osada, S., Suzuki, A., Mizuno, K., and Ohno, S. Protein kinase C activates the MEK-ERK pathway in a manner independent of Ras and dependent on Raf. J. Biol. Chem., *271:* 23512–23519, 1996.
46. Hausser, A., Storz, P., Hubner, S., Braendlin, I., Martinez-Moya, M., Link, G., and Johannes, F. J. Protein kinase Cμ selectively activates the mitogen-activated protein kinase (MAPK) p42 pathway. FEBS Lett, *492:* 39–44, 2001.
47. Keshamouni, V. G., Mattingly, R. R., and Reddy, K. B. Mechanism of 17-β-estradiol-induced Erk1/2 activation in breast cancer cells. A role for HER2 AND PKC-δ. J. Biol. Chem., *277:* 22558–22565, 2002.
48. Stoica, A., Saceda, M., Doraiswamy, V. L., Coleman, C., and Martin, M. B. Regulation of estrogen receptor α gene expression by epidermal growth factor. J. Endocrinol., *165:* 371–378, 2000.
49. Wu, R. C., Qin, J., Hashimoto, Y., Wong, J., Xu, J., Tsai, S. Y., Tsai, M. J., and O'Malley, B. W. Regulation of SRC-3 (pCIP/ACTR/AIB-1/RAC-3/TRAM-1) Coactivator activity by I κ B kinase. Mol. Cell. Biol., *22:* 3549–3561, 2002.
50. Levin, E. R. Cellular functions of the plasma membrane estrogen receptor. Trends Endocrinol. Metab., *10:* 374–377, 1999.
51. Wehling, M. Specific, nongenomic actions of steroid hormones. Annu. Rev. Physiol., *59:* 365–393, 1997.
52. Collins, P., and Webb, C. Estrogen hits the surface. Nat. Med., *5:* 1130–1131, 1999.
53. Flototto, T., Djahansouzi, S., Glaser, M., Hanstein, B., Niederacher, D., Brumm, C., and Beckmann, M. W. Hormones and hormone antagonists: mechanisms of action in carcinogenesis of endometrial and breast cancer. Horm. Metab. Res., *33:* 451–457, 2001.
54. Filardo, E. J., Quinn, J. A., Frackelton, A. R., Jr., and Bland, K. I. Estrogen action via the G protein-coupled receptor, GPR30: stimulation of adenylyl cyclase and cAMP-mediated attenuation of the epidermal growth factor receptor-to-MAPK signaling axis. Mol. Endocrinol., *16:* 70–84, 2002.
55. Sigurdsson, H., Baldetorp, B., Borg, A., Dalberg, M., Ferno, M., Killander, D., and Olsson, H. Indicators of prognosis in node-negative breast cancer. N. Engl. J. Med., *322:* 1045–1053, 1990.
56. Zajchowski, D. A., Bartholdi, M. F., Gong, Y., Webster, L., Liu, H. L., Munishkin, A., Beauheim, C., Harvey, S., Ethier, S. P., and Johnson, P. H. Identification of gene expression profiles that predict the aggressive behavior of breast cancer cells. Cancer Res., *61:* 5168–5178, 2001.
57. Malmstrom, P., Bendahl, P. O., Boiesen, P., Brunner, N., Idvall, I., and Ferno, M. S-phase fraction and urokinase plasminogen activator are better markers for distant recurrences than Nottingham Prognostic Index and histologic grade in a prospective study of premenopausal lymph node-negative breast cancer. J. Clin. Oncol., *19:* 2010–2019, 2001.